Consistent analysis of fusion data without adjustable parameters for systems involving odd nuclei

G. P. A. Nobre, C. P. Silva, and L. C. Chamon
Departamento de Física Nuclear, Instituto de Física da Universidade de São Paulo, Caixa Postal 66318, 05315-970, São Paulo, SP, Brazil

B. V. Carlson
Departamento de Física, Instituto Tecnológico de Aeronáutica, Centro Técnico Aeroespacial, São José dos Campos, SP, Brazil
(Received 3 May 2007; published 14 August 2007)

In a recent article, we calculated fusion cross sections for systems involving even-even nuclei based on a method that takes into account the couplings to a complete set of states for surface vibrations of the nuclear densities. The predictions were obtained without using any adjustable parameter, and are in good agreement with the experimental results for most of the systems, even at sub-barrier energies. In the present work, we extend these calculations to systems involving nuclei with odd number of protons and/or of neutrons.

DOI: 10.1103/PhysRevC.76.024605 PACS number(s): 25.60.Pj, 25.70.Jj

I. INTRODUCTION

Tunneling of a particle through a barrier is a quite general and important subject in many areas of physics. For energies near the barrier height, the potential can be approximated by a parabola and, if no couplings are present, the corresponding transmission coefficient is well known [1]. When dealing with a complex, many-particle system, such as a nucleus, couplings with internal degrees of freedom may significantly affect the transmission mainly at sub-barrier energies (for a review, see Ref. [2]). Although from a theoretical point of view the coupled-channels (CC) formalism is appropriate to describe the heavy-ion fusion, in some cases numerical problems may occur in the solution of the CC equations resulting in unreliable theoretical cross sections, mainly at extreme sub-barrier energies, when a large number of channels is included in the calculations (see, e.g., Refs. [3,4]). In most works that deal with fusion data analyses, a few adjustable parameters related to the bare potential and/or coupling amplitudes were used to fit the data. Despite the good data description generally obtained, this procedure may result in unrealistic values for the free parameters that could hide some particular characteristic of the system [3].

In a recent article [3], we proposed a model, that we call the zero point motion (ZPM) model, where we considered the effect of the couplings to the complete sets of inelastic states connected to the 2^+ and 3^- vibrational bands of even-even nuclei. Despite the large number of coupled channels, the numerical convergence of our calculations is quite good. The analyses were performed in the context of the ZPM model and using the São Paulo (SP) potential [5–7] as the bare interaction. The SP potential has been successful in describing the elastic scattering and peripheral reaction channels for several systems in a wide energy region, from sub-barrier to intermediate energies [6,8–25]. Therefore, the bare interaction assumed to analyze the fusion data is also appropriate to describe the elastic scattering process. In that work [3], we analyzed fusion data for 64 different heavy-ion systems without using any adjustable parameter. At extreme sub-barrier energies (about 20 MeV below the barrier), the unidimensional barrier penetration model (BPM) underestimates the data by about 11 orders of magnitude, whereas the results of the ZPM model agree with the data within about two orders of magnitude for most of the systems. This is an important result due to the lack of adjustable parameters.

In Ref. [3], we considered only systems involving even-even nuclei, because the ZPM model is based on the characteristics (deformation parameter and excitation energy) of the 2^+ and 3^- excited states of the nuclei. In the present work, we extend the ZPM calculations to the fusion of systems involving nuclei with odd number of protons and/or of neutrons (hereafter we call these nuclei simply odd nuclei). To reach this goal, in Sec. II we present a systematics of 2^+ and 3^- excitation energies for even-even nuclei. In Sec. III, we present a brief description of the ZPM model and SP interaction. We use the results of the systematics presented in Sec. II to analyze fusion data in Sec. IV. Section V is devoted to our main conclusions.

In Refs. [3,4], we used the same name, ZPM model, for two different approaches to the heavy-ion fusion problem. This, of course, is a procedure that can lead only to confusion, but, unfortunately, it is what we did. In this work, we use the model presented in Ref. [3] and, to avoid even further confusion, we maintain the name ZPM model for the model assumed here.

II. QUADRUPOLE AND OCTUPOLE EXCITATION ENERGY SYSTEMATICS

In an earlier article [7], we presented an extensive systematics for the densities of heavy nuclei, based on studies of experimental charge distributions and theoretical densities calculated in a Dirac-Hartree-Bogoliubov model. In that work, we adopted a spherically symmetric two-parameter Fermi (2pF) distribution to describe the nuclear densities. We found that the radii of the charge and matter distributions can be well described by

$$R_{0c} = 1.76Z^{1/3} - 0.96 \text{ fm}, \quad (1)$$

$$R_{0m} = 1.31A^{1/3} - 0.84 \text{ fm}, \quad (2)$$

where Z and A are the number of protons and nucleons of the nucleus, respectively. The charge and matter densities present

 ©2007 The American Physical Society

average diffuseness values of $a = 0.53$ fm and $a = 0.56$ fm, respectively. Due to specific nuclear structure effects (single particle and/or collective), the radius and diffuseness parameters show small variations around the corresponding average values throughout the periodic table. In Ref. [7], these variations were analyzed and standard deviations of $\sigma_R = 0.07$ fm and $\sigma_a = 0.025$ fm, relative to the average radius and diffuseness values, respectively, were found. So, it is possible to treat R_{0m} and a as adjustable parameters to fit fusion data. However, this procedure is justified only when the resulting values for these parameters are within certain acceptable ranges. In Ref. [7], we also defined the matter density of the nucleus as a folding of the nucleon distribution of the nucleus with the intrinsic matter density of the nucleon. Thus, we distinguish the matter density from the nucleon distribution by taking into account the finite size of the nucleon.

In another work [26], with the aim of obtaining the deformation parameters, we used the systematics for the quadrupole $B(E2)$ and octupole $B(E3)$ transition probabilities of even-even nuclei from [27,28]. We defined the corresponding deformation lengths by $\delta_\lambda = \beta_\lambda R_{0c}$ and we assumed the following connection with the transition probabilities:

$$B(E\lambda) = \left(\frac{3Ze\beta_\lambda R_{0c}^\lambda}{4\pi}\right)^2. \quad (3)$$

We proposed that the deformation lengths can approximately be described using the following functions:

$$\delta_\lambda = D_\lambda(Z) + D_\lambda(N), \quad (4)$$

where Z and N are the number of protons and neutrons of the nucleus, $D_3(X) = \frac{\alpha}{\sqrt{X}}$ with $\alpha = 3.2$ fm, and the function $D_2(X)$ was given in Table 1 of Ref. [26]. Equation (4) describes the complete set of experimentally extracted deformation lengths with a dispersion (standard deviation) of 0.2 fm (about 15% precision). This precision is only slightly greater than the average experimental uncertainty.

To obtain a systematics for the excitation energies, we adopt a similar procedure as that assumed in Ref. [26] for the deformation parameters. Figures 1 and 2 show the excitation energies of the 2^+ and 3^- excited states for even-even nuclei, obtained in Refs. [27,28], as a function of the number of protons or neutrons of the nuclei. An inspection of Figs. 1 and 2 shows a very interesting similarity between the behavior of the E_λ^* values as a function of Z and N. With the purpose of emphasizing this behavior, we calculated average values over isotopes and also over isotones (Figs. 3 and 4). Based on these findings, very similar to those obtained for deformation parameters [26], we propose that the excitation energies, E_2^* and E_3^*, can approximately be described using the following functions:

$$E_\lambda^* = E_\lambda(Z) + E_\lambda(N). \quad (5)$$

From the fit of the experimental E_λ^* we obtained such functions, which are illustrated in Fig. 5 and presented in Tables I and II. Equation (5), with the functions of Tables I and II, describes the complete set of experimental excitation energies with a dispersion (standard deviation) of 0.30 MeV. This value is much larger than the experimental uncertainties, but it is reasonably precise for the purpose of describing the fusion process through the procedure presented in Sec. IV.

TABLE I. Values of the function $E_2(X)$.

X	E_2 (MeV)	X	E_2 (MeV)	X	E_2 (MeV)	X	E_2 (MeV)
2	0.52	42	0.16	82	1.02	122	0.13
4	1.28	44	0.19	84	0.57	124	0.07
6	2.09	46	0.33	86	0.36	126	0.91
8	3.46	48	0.46	88	0.20	128	0.33
10	0.75	50	1.07	90	0.05	130	0.11
12	0.50	52	0.53	92	0.04	132	−0.02
14	1.11	54	0.29	94	0.02	134	−0.08
16	1.12	56	0.20	96	0.00	136	−0.04
18	0.98	58	0.18	98	−0.01	138	0.01
20	1.20	60	0.15	100	−0.02	140	0.04
22	0.53	62	0.11	102	−0.03	142	0.04
24	0.37	64	0.09	104	−0.04	144	0.04
26	0.42	66	0.09	106	−0.03	146	0.04
28	1.00	68	0.10	108	−0.04	148	0.04
30	0.50	70	0.10	110	−0.03	150	0.05
32	0.45	72	0.12	112	−0.01	152	0.04
34	0.40	74	0.14	114	0.02	154	0.06
36	0.43	76	0.17	116	0.04		
38	0.46	78	0.30	118	0.05		
40	0.38	80	0.44	120	0.11		

III. SP POTENTIAL AND ZPM MODEL

In this section we provide a brief description of the SP potential and ZPM model. Further details can be obtained in Refs. [3,7,26,29].

TABLE II. Values of the function $E_3(X)$.

X	E_3 (MeV)	X	E_3 (MeV)	X	E_3 (MeV)	X	E_3 (MeV)
2	23.7	42	1.11	82	1.31	122	1.26
4	3.30	44	1.24	84	0.77	124	1.46
6	4.07	46	1.41	86	0.53	126	1.47
8	2.66	48	1.45	88	0.28	128	0.56
10	2.49	50	1.73	90	0.31	130	0.51
12	3.45	52	1.42	92	0.39	132	0.19
14	3.34	54	1.21	94	0.43	134	0.04
16	2.43	56	0.92	96	0.57	136	0.01
18	2.08	58	0.80	98	0.47	138	0.05
20	1.76	60	0.73	100	0.48	140	0.26
22	1.60	62	0.63	102	0.37	142	0.46
24	1.99	64	0.60	104	0.51	144	0.29
26	2.20	66	0.63	106	0.53	146	0.29
28	2.57	68	0.93	108	0.58	148	0.40
30	1.85	70	0.85	110	0.47	150	0.28
32	1.47	72	0.79	112	0.47	152	0.51
34	1.31	74	0.79	114	0.50	154	0.40
36	1.20	76	0.94	116	0.46		
38	1.02	78	0.88	118	0.68		
40	1.01	80	1.15	120	1.00		

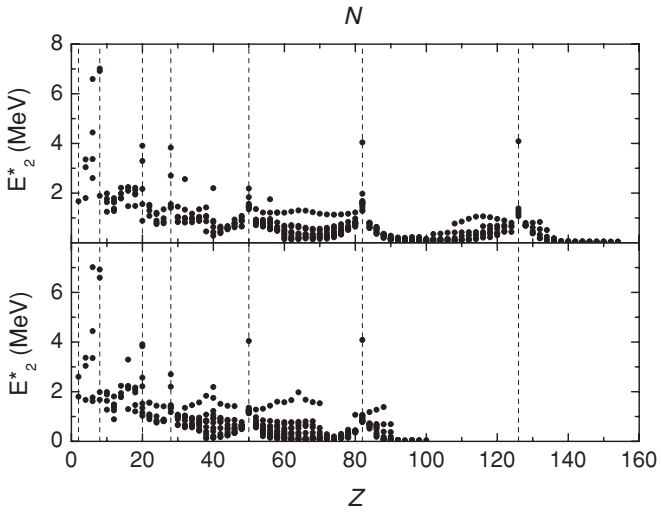

FIG. 1. The values of the experimental excitation energies of the 2^+ state as a function of the number of protons (bottom) or neutrons (top) of the nuclei. The dotted lines represent the magic numbers.

In the present work, we use the SP interaction generalized for deformed nuclei [26,29]. Within this model, the nuclear interaction is connected with the folding potential through [7]:

$$V_N(R, E) = V_F(R)e^{-4V^2/c^2}, \tag{6}$$

where c is the speed of light and V is the local relative velocity between the two nuclei. The folding potential depends on the matter densities of the nuclei involved in the collision:

$$V_F(R) = \int \rho_1(\vec{r}_1)\rho_2(\vec{r}_2)V_0\,\delta(\vec{R} - \vec{r}_1 + \vec{r}_2)d\vec{r}_1 d\vec{r}_2, \tag{7}$$

with $V_0 = -456$ MeV fm^3.

Figure 6 shows a schematic representation of the collision of two deformed nuclei, where θ would represent the direction of the symmetry axis of the nucleus and $\vec{R}$ connects the center of mass of both nuclei. Figure 7 represents the

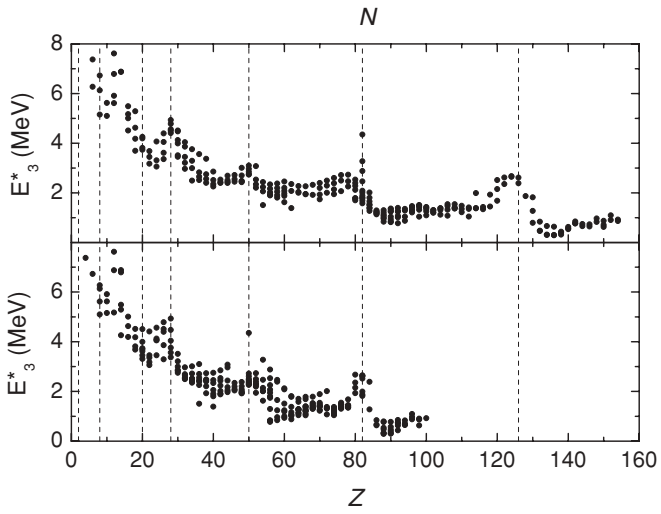

FIG. 2. The values of the experimental excitation energies of the 3^- state as a function of the number of protons (bottom) or neutrons (top) of the nuclei. The dotted lines represent the magic numbers.

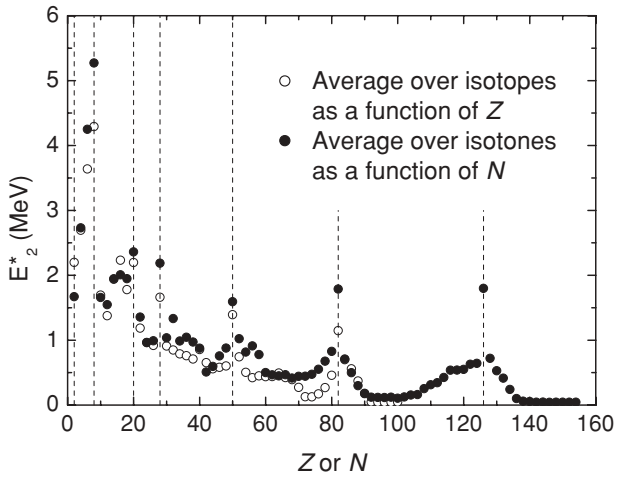

FIG. 3. The average values for isotopes (or isotones) of the 2^+ excitation energies as a function of the number of protons (or neutrons) of the nuclei.

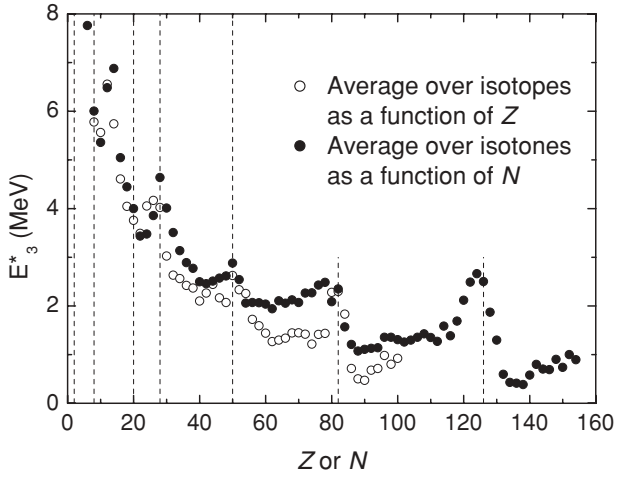

FIG. 4. The average values for isotopes (or isotones) of the 3^- excitation energies as a function of the number of protons (or neutrons) of the nuclei.

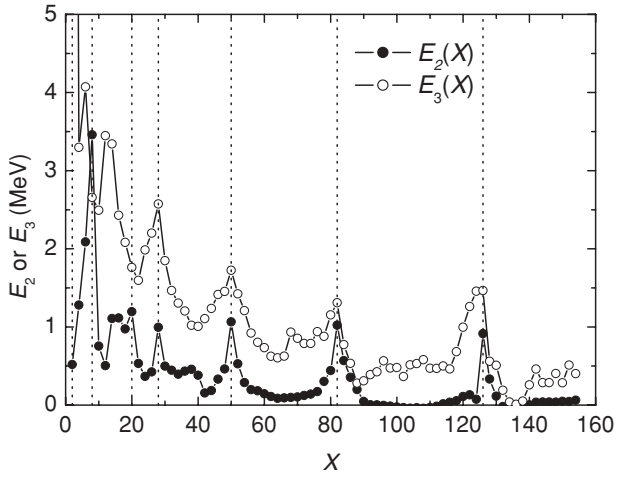

FIG. 5. The functions E_2 and E_3 that approximately describe the behavior of the excitation energies. The dotted lines represent the magic numbers.

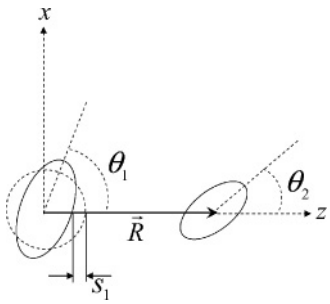

FIG. 6. Schematic representation of the collision between two deformed nuclei. The s coordinate represents the variation of the nuclear radius relative to the spherical shape in the direction of $\vec{R}$.

s-wave effective potentials for an hypothetical system, obtained considering spherical or deformed densities. A parabolic representation of the spherical potential, with barrier height V_B and curvature

$$\hbar\omega = \left|\frac{\hbar^2}{\mu}\frac{d^2V_{\rm eff}}{dR^2}\right|^{1/2}_{R_B}, \tag{8}$$

is also presented in Fig. 7. The main effect of the deformation is a shift in the barrier height, represented in Fig. 7 by ΔV_B, whereas the change in the barrier curvature is small. Due to the short range of the nuclear interaction, the barrier height practically depends only on the coordinate s represented in Fig. 6. Different sets of θ and β values that result in the same s value also provide similar V_B values. For small s values, one can consider the expansion: $V_B(s) = V_{B0} - Fs$, where $V_{B0} = V_B(s = 0)$ and

$$F = -\frac{\partial V_B}{\partial s}. \tag{9}$$

Dasso, Landowne, and Winther [30] obtained the transmission coefficient for a parabolic barrier coupled to a harmonic degree of freedom through a very simple analytical expression. In Ref. [3], within the ZPM model, we generalized this expression to the case of four harmonic degrees of freedom in the context of heavy-ion collisions with the SP potential as the bare interaction. In this context, the collision of two deformed nuclei involves four vibrational coordinates corresponding to the quadrupole and octupole modes of both nuclei. For each

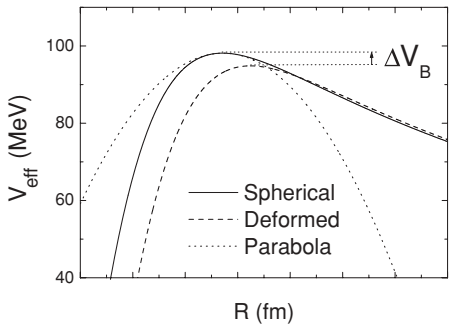

FIG. 7. Effective (sum of nuclear and Coulomb) potentials obtained considering spherical or deformed densities of the nuclei and parabolic representation of the spherical potential. The shift in the barrier height (ΔV_B) is indicated in the figure.

partial wave, the transmission coefficient can be obtained from:

$$T = \sum_{n1}\sum_{n2}\sum_{n3}\sum_{n4} W^{(1)}_{n1}W^{(2)}_{n2}W^{(3)}_{n3}W^{(4)}_{n4}T_n, \tag{10}$$

where the weighting factors are

$$W^{(j)}_n = \frac{1}{n!}\left(\frac{F_j\sigma_j}{E^*_j}\right)^{2n} e^{-(F_j\sigma_j/E^*_j)^2}. \tag{11}$$

The partial transmission coefficients can be obtained through the Hill-Wheeler expression [1]

$$T_n = \frac{1}{1+\exp\left[2\pi\frac{\left(V_B - E + \lambda^{(1)}_{n1} + \lambda^{(2)}_{n2} + \lambda^{(3)}_{n3} + \lambda^{(4)}_{n4}\right)}{\hbar w}\right]}, \tag{12}$$

considering the corresponding eigenvalues

$$\lambda^{(j)}_n = nE^*_j - (F_j\sigma_j)^2/E^*_j. \tag{13}$$

In these expressions, F_j, E^*_j, and σ_j are, respectively, the coupling amplitudes, excitation energies and standard deviations of the four oscillators. The standard deviation of the s-coordinate is connected with the corresponding β value through:

$$\sigma = \frac{\beta R_0}{\sqrt{4\pi}}. \tag{14}$$

As an approximation, we assumed that the F_j are independent parameters and the partial derivative involved in Eq. (9) has been calculated with respect to the spherical shape, i.e., assuming $\theta = 0$ (see Fig. 6) and considering all other β values equal zero. In the more realistic cases where the form factors are rapidly varying with the distance, $F(R) = \partial V_{\rm eff}(R)/\partial s$, the constant-coupling approximation can overestimate low-energy fusion rates [31]. In fact, within the constant-coupling approximation, the barrier radius results in a fixed position. However, due to the R dependence of F, the barrier radius depends on the deformation of the potential. To avoid this problem, we obtained the barrier heights of the deformed potential at the appropriate corresponding barrier radii, considering four configurations: $+2\beta$, $+\beta$, $-\beta$, and -2β. Then, the following derivative is calculated numerically:

$$\frac{\partial V_B}{\partial\beta} \approx \frac{-V_B(2\beta) + 8V_B(\beta) - 8V_B(-\beta) + V_B(-2\beta)}{12\beta}. \tag{15}$$

The strengths are then obtained from:

$$F = -\frac{\partial V_B}{\partial s} = -\frac{\frac{\partial V_B}{\partial\beta}}{R_0 Y_{\lambda 0}(\theta = 0)}. \tag{16}$$

IV. COMPARISON BETWEEN THEORETICAL AND EXPERIMENTAL FUSION CROSS SECTIONS

In Ref. [3], the ZPM model has been applied to analyze fusion data of 64 systems involving only even-even nuclei. The β values of the vibration modes were connected, through Eq. (3), with the corresponding experimental transition amplitudes of quadrupole, $B(E2)$, and octupole, $B(E3)$, obtained in Refs. [27,28]. Also the excitation energies of the 2^+ and 3^-

states were obtained in the same references. In that work [3], the SP interaction was assumed in its standard form, i.e., considering the average parameter values for the nuclear densities [Eq. (2) for the radius and $a = 0.56$ fm for the diffuseness]. In this context, the SP potential has no adjustable parameter and, therefore, the results for theoretical fusion cross sections represent predictions rather than simply data fits. The main results obtained in that work [3] are the following. At extreme sub-barrier energies (about 20 MeV below the barrier), the undeformed BPM underestimates the fusion data by about 11 orders of magnitude, whereas the results of the ZPM model agree with the data within only 2 orders of magnitude for most of the systems. Taking into account the lack of adjustable parameters, the overall agreement between fusion data and theoretical ZPM predictions could be considered quite satisfactory. Of course, there is room for variation in the bare potential to obtain a better agreement between data and theoretical cross sections. In fact, we demonstrated that significant improvement of the data description can be obtained if adjustable parameters related to coupling amplitudes and/or nuclear densities are assumed to fit the data. However, this procedure is justified only when the resulting values for these parameters are within certain acceptable ranges. Indeed, we showed that even an apparently small variation of the nuclear diffuseness could be unrealistic and could hide a different characteristic of a particular system. This is a very important subject because in many works the bare interaction is related to adjustable parameters. Furthermore, the lack of adjustable parameters establishes a good basis to compare results for very different systems. In this context, particular characteristics in the behavior of the data for different systems can be clearly detected. Another important point discussed in Ref. [3] is that we assumed the vibrational model for all nuclei (within the ZPM model). However, some of the systems that we analyzed involve nuclei that could be better represented by the rotational model. Even so, similar agreement concerning data and theoretical predictions were obtained for all systems. In this sense, the ZPM model seems to be appropriated to describe the fusion also for systems involving rotational nuclei. Probably this feature is due to the fact that Eq. (14) provides the exact result for standard deviations of both vibrational and rotational models.

The purpose of the present work is to extend the ZPM calculations to systems involving odd nuclei. This is based on the idea that odd nuclei should have collective vibrations similar to those of the even-even ones. The analyses were performed without any adjustable parameter, assuming the average radius and diffuseness values for the nuclear densities. To estimate the β and E^* values, we used the systematics presented in Sec. II. We assume Eqs. (4) and (5) and, for odd X values, we interpolated the functions D_λ and E_λ between two neighboring even X values. Of course, this procedure has been applied only for odd nuclei, because for even-even nuclei we assumed the corresponding experimental $B(E2)$, $B(E3)$, E_2^*, and E_3^* values of Refs. [27,28]. The procedure of interpolating parameters is not justified *a priori*, because unpaired particles could affect the collective properties of the nuclei in a nonlinear manner. Even so, we assumed this hypothesis to test it in the description of the fusion process.

TABLE III. The table presents the values of the quadrupole (β_2) and octupole (β_3) deformation parameters and also of the corresponding excitation energies for the nuclei studied in this work.

Nucleus	β_2	E_2^* (MeV)	β_3	E_3^* (MeV)
^{6}Li	3.11	1.80	2.34	27.0
^{7}Li	3.01	2.18	2.18	16.8
^{9}Be	2.15	2.97	1.65	6.98
^{10}B	1.60	3.37	1.40	7.37
^{11}B	1.28	3.77	1.34	7.76
^{14}N	0.56	5.55	1.01	6.73
^{15}N	0.43	6.23	0.97	6.02
^{16}O	0.50	6.92	1.20	6.13
^{17}O	0.48	5.57	0.86	5.23
^{18}O	0.54	1.98	1.10	5.10
^{19}F	0.83	2.86	0.77	5.07
^{27}Al	0.46	1.91	0.55	6.74
^{32}S	0.38	2.23	0.70	5.01
^{36}S	0.32	3.29	0.56	4.19
^{35}Cl	0.32	2.02	0.43	4.34
^{37}Cl	0.24	2.24	0.42	4.02
^{45}Sc	0.32	1.23	0.35	3.66
^{46}Ti	0.37	0.89	0.18	3.06
^{50}Ti	0.21	1.55	0.19	4.41
^{51}V	0.25	1.45	0.31	4.37
^{59}Co	0.25	1.16	0.27	3.85
^{58}Ni	0.21	1.45	0.24	4.48
^{60}Ni	0.24	1.33	0.26	4.04
^{62}Ni	0.23	1.17	0.25	2.75
^{64}Ni	0.22	1.35	0.26	3.56
^{65}Cu	0.26	1.18	0.25	3.42
^{70}Ge	0.26	1.04	0.33	2.56
^{73}Ge	0.29	0.72	0.23	2.53
^{74}Ge	0.33	0.60	0.19	2.54
^{76}Ge	0.32	0.56	0.19	2.69
^{89}Y	0.14	1.49	0.19	2.74
^{92}Zr	0.12	0.93	0.21	2.34
^{93}Nb	0.20	0.80	0.18	2.48
^{101}Ru	0.28	0.37	0.17	2.10
^{103}Rh	0.26	0.44	0.17	2.13
^{105}Pd	0.25	0.50	0.17	2.18
^{112}Sn	0.14	1.26	0.15	2.36
^{144}Sm	0.10	1.66	0.17	1.81
^{159}Tb	0.37	0.09	0.12	1.04
^{165}Ho	0.39	0.08	0.12	1.25
^{208}Pb	0.06	4.08	0.13	2.61
^{209}Bi	0.014	1.71	0.10	2.51
^{232}Th	0.30	0.05	0.10	0.77

In Table III, we present the nuclei involved in the 48 systems studied in the present work, with the corresponding β and E^* values assumed for the quadrupole and octupole modes. Figures 8 to 17 and 20 and 21 present the fusion data (from references provided in the captions) and corresponding results of the undeformed BPM (dashed lines) and the ZPM (solid lines) calculations. The energy scale is represented relative to the undeformed s-wave barrier height (V_B). The figures have the same energy and cross-section scales. This procedure

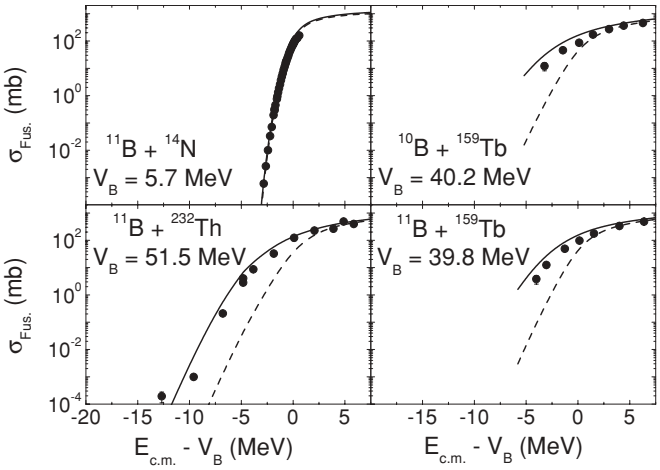

FIG. 8. Fusion data (from Refs. [32–34]) and corresponding undeformed BPM (dashed lines) and ZPM (solid lines) theoretical cross sections for the ^{10}B+^{159}Tb, ^{11}B+^{14}N, ^{159}Tb, and ^{232}Th systems. The s-wave barrier heights of the undeformed potential are presented in the figure.

makes the comparison among results of different systems simple.

Figure 8 presents data of systems involving ^{10,11}B as projectiles. For the light ^{11}B+^{14}N system, the ZPM and BPM results are almost indistinguishable and agree quite precisely with the data in the entire energy region. For the heavier systems, significant enhancements of the data relative to BPM calculations can be observed, whereas the agreement between data and ZPM results is quite reasonable. Figures 9 to 11 present systems involving nitrogen, fluorine, oxygen, and aluminum isotopes as projectiles. A quite reasonable agreement between data and ZPM results is observed for all systems. Figures 12 to 16 show systems involving sulfur and chlorine isotopes as projectiles and, again, quite reasonable predictions of the ZPM model are obtained, with some disagreement observed for ^{36}S (see Fig. 13). Figure 17 presents the heaviest systems studied in this work, and only for

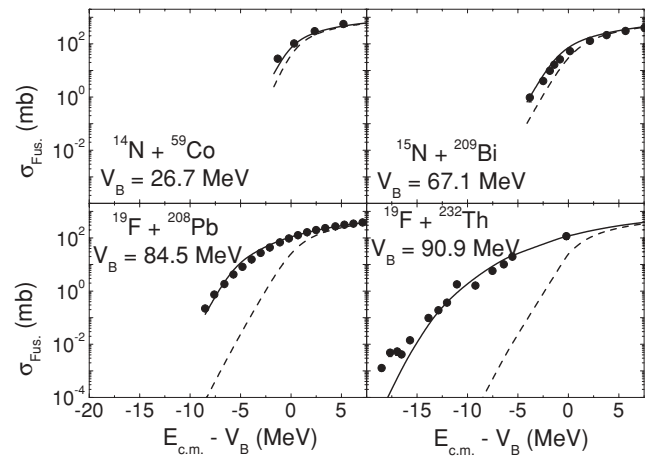

FIG. 9. The same as in Fig. 8 for the systems indicated in the figure. The data are from Refs. [33,35–37].

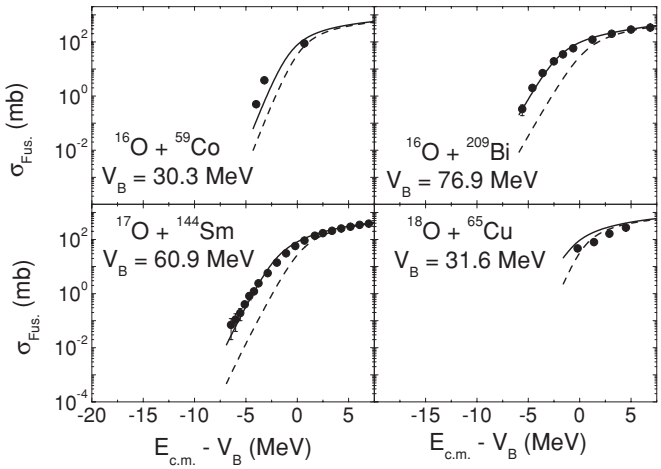

FIG. 10. The same as in Fig. 8 for the systems indicated in the figure. The data are from Refs. [35,36,38,39].

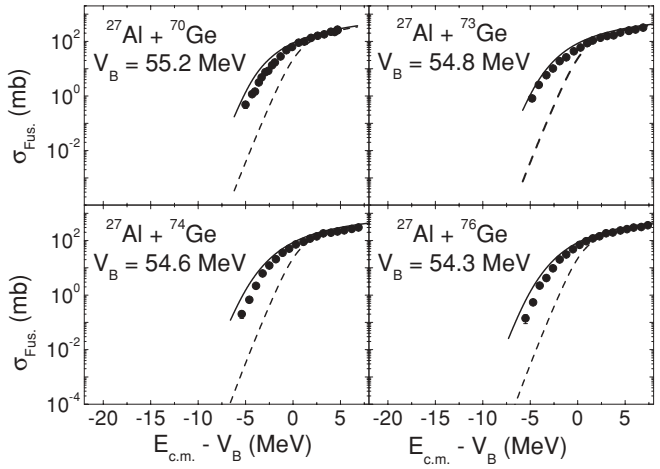

FIG. 11. The same as in Fig. 8 for the systems indicated in the figure. The data are from Ref. [40].

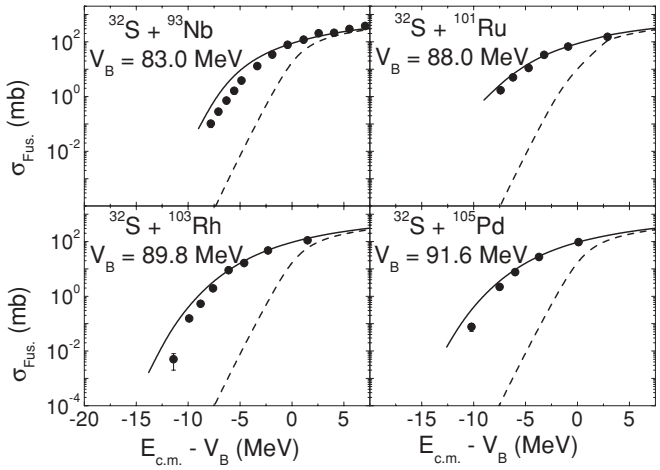

FIG. 12. The same as in Fig. 8 for the systems indicated in the figure. The data are from Refs. [41,42].

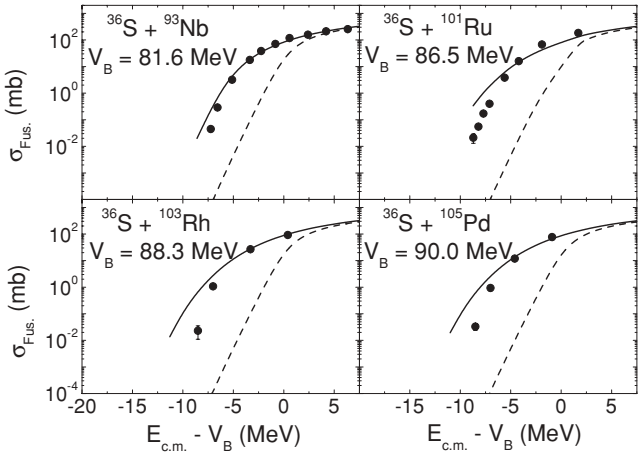

FIG. 13. The same as in Fig. 8 for the systems indicated in the figure. The data are from Refs. [41,42].

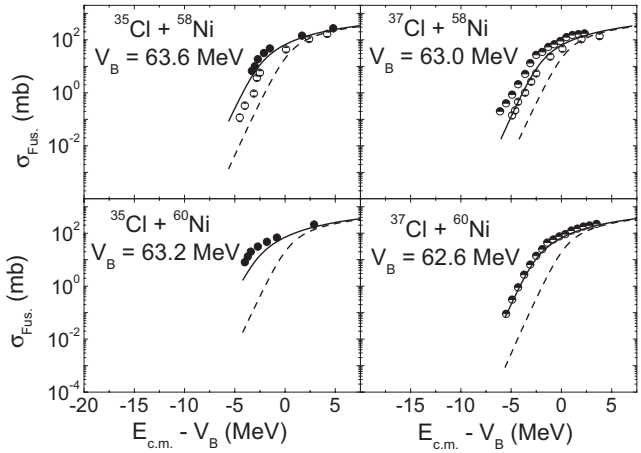

FIG. 14. The same as in Fig. 8 for the systems indicated in the figure. The data are from Refs. [43–45]. There are different data sets (indicated by different symbols) with measured cross sections that can significantly differ from each other.

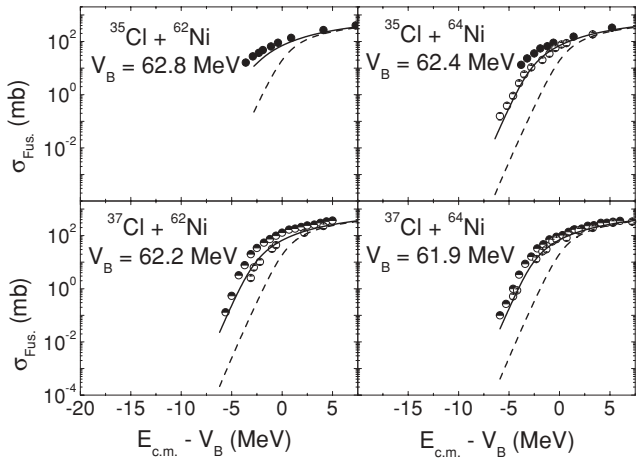

FIG. 15. The same as in Fig. 8 for the systems indicated in the figure. The data are from Refs. [43–45]. There are different data sets (indicated by different symbols) with measured cross sections that can significantly differ from each other.

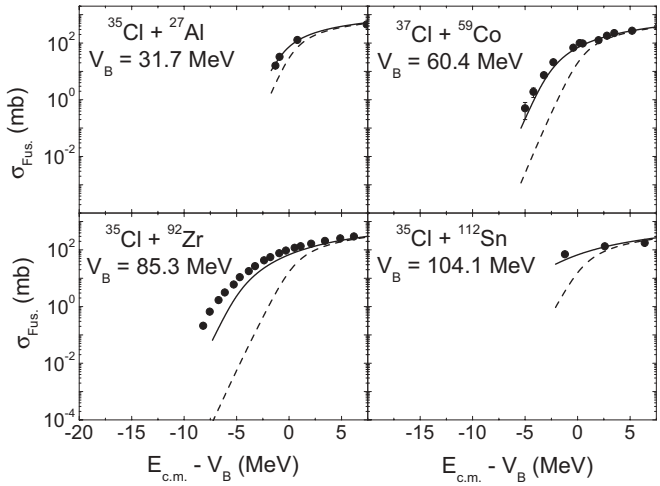

FIG. 16. The same as in Fig. 8 for the systems indicated in the figure. The data are from Refs. [43,46–48].

^{60}Ni+^{89}Y is the ZPM model not so precise in describing the sub-barrier data.

In Fig. 18, we present a summary of the results shown in Figs. 8 to 17, by calculating the ratio between fusion data and corresponding BPM or ZPM cross sections. For comparison purpose, the figure also contains the results for systems involving only even-even nuclei. We warn the reader that, in the case of the even-even nuclei, we included in Fig. 18 data for ^{40}Ca+^{192}Os, ^{116}Sn, and ^{40}Ar+^{116}Os, which were not included in a similar figure presented in Ref. [3]. At extreme sub-barrier energies, the data are underestimated by the BPM calculations by 11 orders of magnitude (see Fig. 18). However, the ZPM cross sections agree with the data within about 2 orders of magnitude for almost all the systems. One should observe in Fig. 18 that no significant difference between the results for systems involving odd and only even-even nuclei is observed. This indicates that the procedure of interpolating β_λ and E^*_λ values for odd nuclei is appropriate for describing the fusion process.

In Fig. 19 (top), we present the ratio between fusion data and ZPM cross sections for the complete set of odd

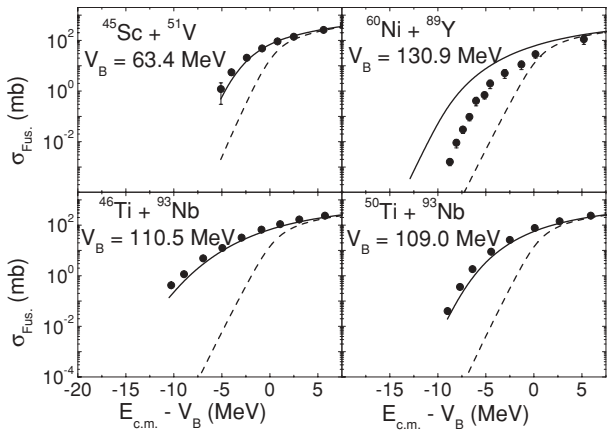

FIG. 17. The same as in Fig. 8 for the systems indicated in the figure. The data are from Refs. [41,46,49].

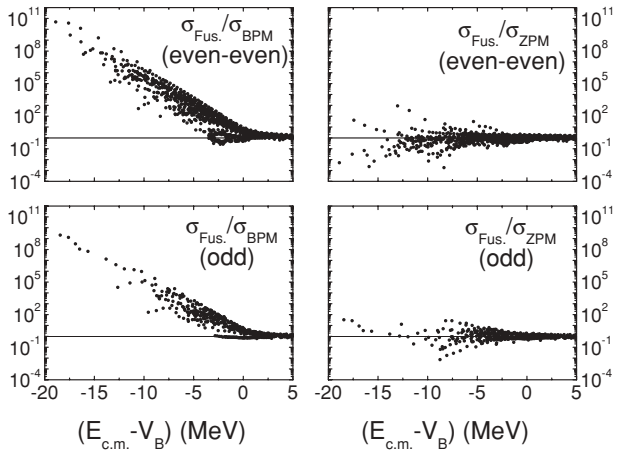

FIG. 18. Ratio between fusion data and BPM (left side) or ZPM (right side) theoretical cross sections for systems involving odd (bottom panels) or even-even (top panels) nuclei.

and even-even nuclei. As a first impression, the precision of two orders of magnitude that the ZPM model describes the data at low energies could seem unsatisfactory. However, one should realize the following comments. No free parameters were assumed in our ZPM calculations, but the β values for even-even nuclei were obtained from the experimental $B(E\lambda)$, which have experimental uncertainties. For odd nuclei, the β and E^* values were obtained from interpolation and, therefore, the "uncertainties" of these parameters are even larger than those for even-even nuclei. Furthermore, we assumed the average values for the density parameters, but as already commented the radius and diffuseness parameters show small variations around the corresponding average values throughout the periodic table. Therefore, one should expect a spread of

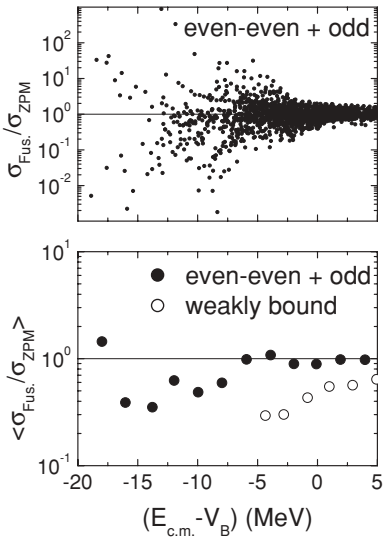

FIG. 19. (Top) Ratio between fusion data and ZPM cross sections for systems involving odd and even-even nuclei. (Bottom) Average values of the order of magnitude of the deviations between fusion data and ZPM cross sections for systems involving odd and even-even nuclei and also for systems involving the weakly bound ^{6,7}Li and ^{9}Be nuclei.

the ZPM results around the fusion data due to the fluctuations of the coupling and density parameters relative to the average values assumed in our calculations. Obviously, this dispersion should be larger at very low energies where the effect of the couplings is more important. This apparently large dispersion of 2 orders of magnitude is, in fact, 9 orders smaller than the effect of the couplings, which reaches 11 orders of magnitude at extreme sub-barrier energies, as can be observed from the difference between fusion data and BPM cross sections.

However, these fluctuations should partially cancel when calculating average values for several systems. To emphasize this point, we obtained average values for the order of magnitude of the deviations between fusion data and ZPM cross sections. We divided the data presented in Fig. 19 (top) in consecutive bins of 2 MeV. For each bin we calculated the average value of $\ln(\sigma_{\text{Fus.}}/\sigma_{\text{ZPM}})$ and defined average values for the order of magnitude through the following expression $\langle\sigma_{\text{Fus.}}/\sigma_{\text{ZPM}}\rangle = e^{\langle\ln(\sigma_{\text{Fus.}}/\sigma_{\text{ZPM}})\rangle}$. The corresponding results are presented in Fig. 19 (bottom). In this figure one can observe that, on average, the ZPM results agree with the fusion data within a factor about 2 in the whole energy region considered in this work. This result is very similar to that presented in Ref. [3], in which only systems involving even-even nuclei were analyzed, except in the region $E_{\text{c.m.}} - V_B < -15$ MeV, where larger discrepancies were found in that work. Thus, one could claim a detected difference between the results for the sets of odd and only even-even nuclei. However, in this low-energy region there are measured fusion data for only five systems and, therefore, the statistics in this energy region is very small [see Fig. 19(top)] that results in large fluctuations of the average values. Thus, we consider that no significant difference between the analyses of the even-even and odd data sets has been detected. Due to the larger number of systems considered here, the results for average values of the present work are probably more precise than those obtained in Ref. [3].

Figures 20 and 21 show systems involving the weakly bound ^{6,7}Li and ^{9}Be nuclei. Here, an important difference relative to the other systems is observed. Clearly, there is a hindrance of the data relative to the ZPM results even

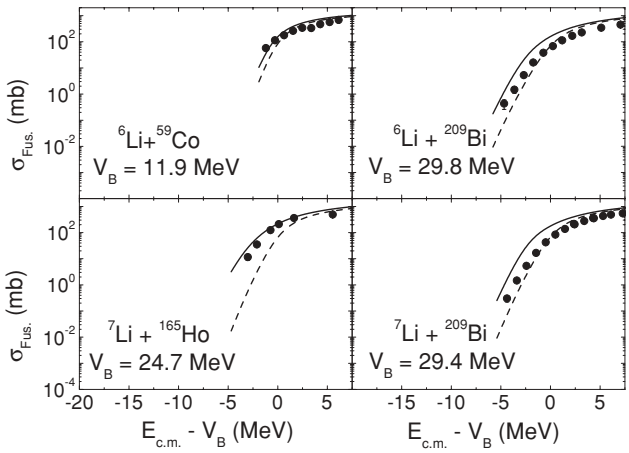

FIG. 20. The same as in Fig. 8 for the systems indicated in the figure. The data are from Refs. [50–52].

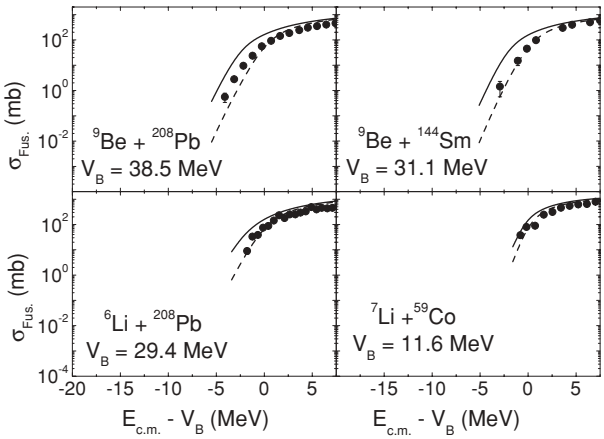

FIG. 21. The same as in Fig. 8 for the systems indicated in the figure. The data are from Refs. [23,50,51,53].

at energies above the barrier. To illustrate this point, the corresponding average values are also presented in Fig. 19 (bottom). A possible explanation for this hindrance is the competition of the breakup process with the fusion that should be significant for systems involving weakly bound nuclei, as already discussed in many works (see, e.g., Refs. [54,55]).

V. SUMMARY AND CONCLUSION

The ZPM model takes into account the effect of the harmonic vibrational modes in the calculation of transmission coefficients, and therefore it describes a large number of couplings to inelastic states. The tunneling process strongly depends on the barrier height, which is related to variations of the distance between the surfaces of the nuclei. Thus, heavy-ion fusion is quite sensitive to vibrations of the nuclear densities. In our calculations, we assumed the SP potential in the context of the systematics for the nuclear densities. Thus, no free parameters were assumed in our analyses. We described fusion data for 48 heavy-ion systems involving odd nuclei, for which the coupling parameters were obtained through the systematics of even-even nuclei. The results obtained here for odd nuclei are similar to those earlier presented for even-even nuclei [3]. Taking into account the lack of adjustable parameters, the overall agreement between fusion data and theoretical ZPM predictions can be considered quite satisfactory, within only 2 orders of magnitude for almost all the systems. Therefore, the large enhancements of the data relative to undeformed BPM calculations are mostly due to the effect of the couplings to inelastic states. Due to the fluctuations of the density and coupling parameters around the corresponding average values assumed in our calculations, one should expect the observed spread of the ZPM cross sections relative to the fusion data, mainly at extreme sub-barrier energies where the effect of the couplings is very large. This dispersion should partially cancel when considering averages over several systems and, in fact, on average the ZPM predictions agree with the data within only a factor about 2 in the whole energy region studied in this work. This precision of a factor of 2 can be considered remarkable, taking into account that the BPM underestimates the data by 11 orders of magnitude at extreme sub-barrier energies. An important exception corresponds to systems involving the weakly bound ^{6,7}Li and ^{9}Be nuclei, where a hindrance of the data relative to the ZPM cross sections has been observed even at above barrier energies. We point out that this behavior could be clearly detected here due to the lack of adjustable parameters of our model. This effect for weakly bound nuclei can be due to the competition of the breakup process with the fusion. Finally, we emphasize that the SP potential has been successful in describing the elastic-scattering process for a large number of systems in a very wide energy range. Therefore, we obtained an important correlation between the analyses of the heavy-ion fusion and elastic-scattering processes. The ZPM calculations were performed using the computational code SPZPM, which is available on request from L. C. Chamon.

ACKNOWLEDGMENTS

This work was partially supported by Financiadora de Estudos e Projetos (FINEP), Fundação de Amparo à Pesquisa do Estado de São Paulo (FAPESP), and Conselho Nacional de Desenvolvimento Científico e Tecnológico (CNPq).

[1] D. L. Hill and J. A. Wheeler, Phys. Rev. **89**, 1102 (1953).
[2] A. B. Balantekin and N. Takigawa, Rev. Mod. Phys. **70**, 77 (1998).
[3] G. P. A. Nobre, L. C. Chamon, L. R. Gasques, B. V. Carlson, and I. J. Thompson, Phys. Rev. C **75**, 044606 (2007).
[4] G. P. A. Nobre, L. C. Chamon, B. V. Carlson, I. J. Thompson, and L. R. Gasques, Nucl. Phys. **A786**, 90 (2007).
[5] M. A. Cândido Ribeiro, L. C. Chamon, D. Pereira, M. S. Hussein, and D. Galetti, Phys. Rev. Lett. **78**, 3270 (1997).
[6] L. C. Chamon, D. Pereira, M. S. Hussein, M. A. Cândido Ribeiro, and D. Galetti, Phys. Rev. Lett. **79**, 5218 (1997).
[7] L. C. Chamon, B. V. Carlson, L. R. Gasques, D. Pereira, C. De Conti, M. A. G. Alvarez, M. S. Hussein, M. A. Cândido Ribeiro, E. S. Rossi Jr., and C. P. Silva, Phys. Rev. C **66**, 014610 (2002).
[8] J. J. S. Alves *et al.*, Nucl. Phys. **A748**, 59 (2005).
[9] D. Pereira, C. P. Silva, J. Lubian, E. S. Rossi Jr., and L. C. Chamon, Phys. Rev. C **73**, 014601 (2006).
[10] L. C. Chamon, D. Pereira, and M. S. Hussein, Phys. Rev. C **58**, 576 (1998).
[11] M. A. G. Alvarez, L. C. Chamon, D. Pereira, E. S. Rossi Jr., C. P. Silva, L. R. Gasques, H. Dias, and M. O. Roos, Nucl. Phys. **A656**, 187 (1999).
[12] L. R. Gasques, L. C. Chamon, C. P. Silva, D. Pereira, M. A. G. Alvarez, E. S. Rossi Jr., V. P. Likhachev, B. V. Carlson, and C. De Conti, Phys. Rev. C **65**, 044314 (2002).
[13] E. S. Rossi Jr., D. Pereira, L. C. Chamon, C. P. Silva, M. A. G. Alvarez, L. R. Gasques, J. Lubian, B. V. Carlson, and C. De Conti, Nucl. Phys. **A707**, 325 (2002).
[14] L. R. Gasques *et al.*, Phys. Rev. C **67**, 024602 (2003).
[15] T. Tarutina, L. C. Chamon, and M. S. Hussein, Phys. Rev. C **67**, 044605 (2003).

[16] M. A. G. Alvarez, L. C. Chamon, M. S. Hussein, D. Pereira, L. R. Gasques, E. S. Rossi Jr., and C. P. Silva, Nucl. Phys. **A723**, 93 (2003).
[17] L. R. Gasques, L. C. Chamon, D. Pereira, M. A. G. Alvarez, E. S. Rossi Jr., C. P. Silva, G. P. A. Nobre, and B. V. Carlson, Phys. Rev. C **67**, 067603 (2003).
[18] P. R. S. Gomes *et al*., Phys. Rev. C **70**, 054605 (2004).
[19] M. A. G. Alvarez, N. Alamanos, L. C. Chamon, and M. S. Hussein, Nucl. Phys. **A753**, 83 (2005).
[20] P. R. S. Gomes *et al*., Phys. Rev. C **71**, 034608 (2005).
[21] J. J. S. Alves *et al*., Braz. J. Phys. **35**, 909 (2005).
[22] P. R. S. Gomes *et al*., J. Phys. G **31**, S1669 (2005).
[23] P. R. S. Gomes *et al*., Phys. Lett. **B634**, 356 (2006).
[24] P. R. S. Gomes *et al*., Phys. Rev. C **73**, 064606 (2006).
[25] J. C. Werner *et al*., Nucl. Phys. **A781**, 342 (2007).
[26] L. C. Chamon, G. P. A. Nobre, D. Pereira, E. S. Rossi Jr., C. P. Silva, L. R. Gasques, and B. V. Carlson, Phys. Rev. C **70**, 014604 (2004).
[27] S. Raman, C. H. Malarkey, W. T. Milner, C. W. Nestor Jr., and P. H. Stelson, At. Data Nucl. Data Tables **36**, 1 (1987).
[28] T. Kibedi and R. H. Spear, At. Data Nucl. Data Tables **80**, 35 (2002).
[29] B. V. Carlson, L. C. Chamon, and L. R. Gasques, Phys. Rev. C **70**, 057602 (2004).
[30] C. H. Dasso, S. Landowne, and A. Winther, Nucl. Phys. **A407**, 221 (1983).
[31] O. Tanimura, J. Makowka, and U. Mosel, Phys. Lett. **B163**, 317 (1985).
[32] B. Dasmahapatra, B. Cujec, and F. Lahlou, Can. J. Phys. **61**, 657 (1983).
[33] D. M. Nadkarni, A. Saxena, D. C. Biswas, R. K. Choudhury, S. S. Kapoor, N. Majumdar, and P. Bhattacharya, Phys. Rev. C **59**, R580 (1999).
[34] A. Mukherjee *et al*., Phys. Lett. **B636**, 91 (2006).
[35] P. R. S. Gomes, T. J. P. Penna, E. F. Chagas, R. Liguori Neto, J. C. Acquadro, P. R. Pascholati, N. Carlin, and M. M. Coimbra, Nucl. Phys. **A534**, 429 (1991).
[36] E. Vulgaris, L. Grodzins, S. G. Steadman, and R. Ledoux, Phys. Rev. C **33**, 2017 (1986).
[37] D. J. Hinde, A. C. Berriman, M. Dasgupta, J. R. Leigh, J. C. Mein, C. R. Morton, and J. O. Newton, Phys. Rev. C **60**, 054602 (1999).
[38] J. R. Leigh *et al*., Phys. Rev. C **52**, 3151 (1995).
[39] L. C. Chamon, D. Pereira, E. S. Rossi, C. P. Silva, G. R. Razeto, A. M. Borges, L. C. Gomes, and O. Sala, Phys. Lett. **B275**, 29 (1992).
[40] E. F. Aguilera, J. J. Vega, J. J. Kolata, A. Morsad, R. G. Tighe, and X. J. Kong, Phys. Rev. C **41**, 910 (1990).
[41] P. H. Stelson, H. J. Kim, M. Beckerman, D. Shapira, and R. L. Robinson, Phys. Rev. C **41**, 1584 (1990).
[42] R. Pengo, D. Evers, K. E. G. Lobner, U. Quade, K. Rudolph, S. J. Skorka, and I. Weidl, Nucl. Phys. **A411**, 255 (1983).
[43] W. Scobel, H. H. Gutbrod, M. Blann, and A. Mignerey, Phys. Rev. C **14**, 1808 (1976).
[44] S. J. Skorka *et al*., Z. Phys. A **328**, 355 (1987).
[45] J. J. Vega, E. F. Aguilera, G. Murillo, J. J. Kolata, A. Morsad, and X. J. Kong, Phys. Rev. C **42**, 947 (1990).
[46] M. Dasgupta, A. Navin, Y. K. Agarwal, C. V. K. Baba, H. C. Jain, M. L. Jhingan, and A. Roy, Nucl. Phys. **A539**, 351 (1992).
[47] J. O. Newton, C. R. Morton, M. Dasgupta, J. R. Leigh, J. C. Mein, D. J. Hinde, H. Timmers, and K. Hagino, Phys. Rev. C **64**, 064608 (2001).
[48] P. David, J. Bisplinghoff, M. Blann, T. Mayer-Kuckuk, and A. Mignerey, Nucl. Phys. **A287**, 179 (1977).
[49] C. L. Jiang *et al*., Phys. Rev. Lett. **89**, 052701 (2002).
[50] C. Beck *et al*., Phys. Rev. C **67**, 054602 (2003).
[51] M. Dasgupta *et al*., Phys. Rev. C **70**, 024606 (2004).
[52] V. Tripathi, A. Navin, K. Mahata, K. Ramachandran, A. Chatterjee, and S. Kailas, Phys. Rev. Lett. **88**, 172701 (2002).
[53] Y. W. Wu, Z. H. Liu, C. J. Lin, H. Q. Zhang, M. Ruan, F. Yang, Z. C. Li, M. Trotta, and K. Hagino, Phys. Rev. C **68**, 044605 (2003).
[54] E. Crema, L. C. Chamon, and P. R. S. Gomes, Phys. Rev. C **72**, 034610 (2005).
[55] M. Dasgupta *et al*., Phys. Rev. Lett. **82**, 1395 (1999).